Tracheid dimensions of Norway spruce in uneven-aged stands

List of authors:

Jiri Pyörälä[1)], email: jiri.pyorala@helsinki.fi and

Riikka Piispanen[2)], email: ext.riikka.piispanen@luke.fi

Sauli Valkonen[3)], email: sauli.valkonen@luke.fi

Sven-Olof Lundqvist[4)] email: svenolof.lundqvist@indic.se

For 1) Affiliation: University of Helsinki, Department of Forest Sciences

Address: Latokartanonkaari 7, P.O. Box 27, 00014 University of Helsinki

For 2) and 3) Affiliation: Natural Resources Institute Finland, Luke

Address: Latokartanonkaari 9, P.O. Box 2, FI-00791 Helsinki, Finland

For 4) Affiliation: IIC

Address: Rosenlundsgatan 48B, 11863 Stockholm, Sweden

Corresponding author: Name: Riikka Piispanen

Affiliation: Natural Resources Institute Finland, Luke

Address: Latokartanonkaari 9, P.O. Box 2, FI-00791 Helsinki, Finland

Tel. +358 029 532 5473

e-mail: ext.riikka.piispanen@luke.fi

Abstract

Tracheid length and width patterns from pith to bark at a height of 0.6 m in uneven-aged Norway spruce (*Picea abies* L. (H.) Karst) trees were addressed. The identification of the main factors and a comparison with even-aged stands were also pursued. 96 trees were sampled from experimental stands in Southern Finland. The material encompassed the variation in tracheid properties from early years to silvicultural maturity, i.e. from corewood to outerwood up to a cambial age of 111 years. Data from 39 Norway spruce trees from even-aged stands we utilized for comparison. Models fitted to the data indicated that annual ring widths did not influence mean tracheid dimensions but the latewood proportion showed a significant influence on tracheid dimensions. Tracheids in uneven-aged stands were slightly wider and longer at the base of the stem with a similar tree diameter, cambial age, and annual ring number.

Keywords

Wood properties, Norway spruce, tracheid length, tracheid width, uneven-aged stands

1. Introduction

The management of even-aged stands (EAS) has been the overwhelmingly predominant mode of silviculture in the Nordic countries of Finland, Norway, and Sweden since the 1950s, and contemporary forests are characterized by uniform stands with the predominance of a single species with homogenous spacing, stem diameter, height, and canopy characteristics. Clear-cutting is the main method for forest renewal in EAS used throughout the boreal forest zone. Homogeneous stands and large-scale clear-cuts have been increasingly associated with reducing biodiversity and the loss of various ecosystem functions and services (Gauthier et al. 2015; Boucher et al. 2017; García-Tejero et al. 2018).

In contrast with EAS, ecosystem-based forest management practices such as the management of uneven-aged stands (UAS) are associated with a greater degree of structural heterogeneity which may increase the biodiversity in managed forests (Assmuth and Tahvonen 2018; Nolet et al. 2018). Single-tree and group selection is currently considered the primary UAS method in the management of Norway spruce (*Picea abies* L. (H.) Karst) dominated stands in the Nordic countries. Uneven-aged stands are made up of trees of multiple ages and sizes, mixed at small spatial scales, resulting in complex competitive interactions between the trees. Selection harvesting is applied, targeting mainly large tree individuals that are considered economically mature. Trees are removed individually or in small groups or patches. Trees typically experience consecutive suppression and release phases, especially at early ages (Schütz 2001).

The management of uneven-aged stands is expected to gradually achieve a minor but established status in practical forestry in Nordic boreal forests. There is a great demand for research results on the effects of uneven-aged management on tree growth

and wood formation in comparison to those in EAS. Such information is needed for the development of practical guidelines and management services for uneven-aged methods throughout the boreal forest zone (Puettmann et al. 2015), with respect to the expected quantity and quality of wood products produced.

The primary wood products in uneven-aged management are sawlogs, and the wood properties and quality of logs and sawn timber from UAS has been previously studied (Seeling 2001; Macdonald et al. 2010; Piispanen et al. 2014; Pretzsch and Rais 2016; Pamerleau-Couture et al. 2019; Piispanen et al. 2020). However, a considerable portion of the harvested volume is used for pulp from culled logs that are unsuitable for producing lumber (an average of 33% was reported by Laamanen (2014)), and from chips produced from the outside of the logs during lumber manufacturing (slabs, chips, and sawdust make up approximately 33% of the sawlog volume according to Natural Resources Institute Finland, Statistics database, https://stat.luke.fi/en/, statistics 2018). Tracheid dimensions are important pulp quality indicators that can be used to predict final pulp properties, for instance, the stiffness and coarseness of pulp fibers and density of sheets produced.

The development of tracheid dimensions in xylem exhibits well-established relationships with the cambial aging and radial growth of the stem (Lindström 1997; Fabris 2000; Sirviö and Kärenlampi 2001, Savva et al. 2010). The dependency reflects the processes of wood formation, adapting to changes in water conductivity and mechanical load, regulated through hormonal responses that are also affected by the environment, e.g. silviculture, climate, and canopy position (Schrader et al. 2003; Rathgeber et al. 2011; Sorce et al. 2013). Wood formation and patterns of tracheid size development from pith to bark are in large part genetically encoded (Zobel and Jett 2012), but forest management also influences tree growth and tracheid formation

via its effect on the growth conditions. Due to heterogeneous canopy structures and the repeated removal of neighboring trees in UAS, multiple changes in the ranking of the trees' canopy positions occur throughout the life-cycle of a tree, in contrast with EAS where trees mainly maintain similar canopy positions over the entire rotation. In trees from UAS, reflections of shifting canopy positions can be found in the wood properties. For example, the corewood had narrower annual rings and larger proportions of latewood, while the outermost annual rings were wider and had less latewood (Piispanen et al. 2014). These are likely consequences of slow growth in young trees, suppressed by the older trees, and faster growth in old trees in dominant positions among younger trees. To date, very few studies have investigated tracheid properties in UAS-grown trees (Pamerleau-Couture et al. 2019), and to our knowledge, the effect from early suppression during the corewood production phase on the development of tracheid dimensions from pith to bark has not been studied before.

The objectives of this study were to

1) characterize the patterns of tracheid width and tracheid length along the stem radius (pith-to-bark) in Norway spruce trees in uneven-aged stands;
2) identify the effects of varying growth rates (in terms of ring width, and latewood percentage) of tracheid dimensions along the stem radius;
3) compare the tracheid dimensions between even-aged and uneven-aged management.

2. Materials and Methods

2.1. UAS data source

Sample trees were harvested from permanent UAS experiments belonging to a set of 25 experimental stands at three geographic locations in southern Finland (60.6–62.6 N, 25.1–27.1 E): Lapinjärvi (LAP), Vesijako (VES) and Suonenjoki (SUO). Five stands (LAP01 and 13; VES; SUO03 and 04) were selected for studies of wood properties (Piispanen et al. 2014, 2020 and this study). The selection criteria were: *i*) a balanced coverage of geographic area and site conditions; and *ii*) stand properties resembling those associated with single-tree selection (i.e. balanced spatial and size distribution of vigorous trees). The stands were located on mineral soil and classified as the submesic *Myrtillus* site type, except stand LAP01, which was on a mesic *Oxalis-Myrtillus* site type (Cajander 1949). All were dominated by Norway spruce but also contained admixtures of Scots pine (*Pinus sylvestris* L.) and various broadleaf species, mainly silver birch (*Betula pendula* Roth), downy birch (*Betula pubescens* Ehrh.) and aspen (*Populus tremula* L.) with a 10–50% proportion of volume.

All the stands could at that time be characterized as truly multi-aged (with trees aged up to 170 years present) and full-storied, as defined by Ahlström and Lundqvist (2015). Single-tree selection targeting the maintenance or enhancement of the existing complex stand structures was adopted in the 1980s, and a single-tree selection cutting was carried out in all of the stands in 1985–1988. After the establishment of the experiments in 1991–1996, the selection cutting was repeated in 1996 and 2011 in LAP01 and LAP13, 2007 at VES, and 2008 at SUO03 and SUO04. All trees with defects or damage were removed first, then healthy trees mainly from the larger diameter classes (>25 cm) were removed until a target basal area was achieved.

Each stand comprised an area of 1–2 ha. One experimental plot was placed in the central area of each stand. In LAP01 and LAP13, each stand had only one plot (40 m

× 40 m) with a single basal area level within the plot (14.2 m^2 ha^{-1} for LAP01 and 18.7 for LAP 13, respectively). The stand outside the plot was treated similarly to that inside the plot. In the three stands, VES, SUO03, and SUO04, the plots were larger (80 m × 100 m) and were divided into eight subplots of different basal areas introduce density variation within the stand. A series of four basal area levels was therefore established in two replications on each of these three plots. In VES, the levels were 8, 12, 16, and 20 m^2 ha^{-1}, while in SUO03 and SUO04, they were 10, 15, 20, and 25 m^2ha^{-1}. The subplot sizes were 40 m × 20 m or 40 m × 30 m (edge plots). The stand adjoining the subplot on the outside was harvested similarly to the subplot. The sampling for this study was evenly distributed between subplots to ensure a wide representation of stand densities. More details on silvicultural and experimental issues can be found in Saksa and Valkonen (2011), Eerikäinen et al. (2014), and Hynynen et al. (2019).

A total of 96 Norway spruce trees was sampled (Piispanen et al. (2014),), 32 trees from each experimental stand. The sampling was evenly stratified across subplots in stands where subplots existed (VES, SUO3, SUO4), and the tree diameter classes (or size classes) to ensure even representation. Four trees (eight trees at VES) were taken from each size class (0–9.99 cm, 10–19.99 cm, 20–29.99 cm and > 30 cm stem diameter at breast height). In VES, no trees were available in the size class of 10–19.99 cm on subplots 7 and 8. Consequently, more trees were sampled from subplot 1.

2.2. EAS data source

A combination of existing Finnish and Swedish datasets was used to constitute comparable EAS data. Five stands from southern Sweden were selected, which represented different levels of soil fertility on mineral soil in normal commercial

forests (57.1–57.2N, 14.8–15.3E; plots SWE 1–5) (Piispanen et al. 2014,). Two of the stands were approaching maturity, and three stands had undergone their first commercial thinning. At least 10 years had elapsed since the last thinning, and the stand basal areas (22–30 m^2ha^{-1} with a dominant height of 15–17 m) were consistent with the guidelines for best practices in Finnish Forestry (Rantala 2011). The stands had been planted, except the oldest one (SWE 5), for which the regeneration method was unknown. A circular plot was subjectively placed at a representative point in each stand. The plot size was adjusted to include at least 25 healthy trees (radius 6–12 m). Tree species and stem diameter at breast height were recorded for each tree. On each plot, the cumulative basal area distribution of the trees was divided into three classes of equal size, and one sample tree was randomly chosen from each class. The sample trees had to be healthy, i.e. no visible damage was allowed. 27 trees were sampled.

In Finland, the EAS materials were collected from two thinning experiments in Heinola and Parkano (FIN 6 and FIN 8), in southern Finland (61.2–62.2N, 22.9–26.0E). The stands represented mesic *Oxalis-Myrtillus* and submesic *Myrtillus* site types (Cajander 1949). Experiments FIN 6 and FIN 8 were established in 1970 and 1966, respectively. Both stands had been planted and were at the final cut stage at the time of this study. In both experiments, a plot representing the stand density recommended in best practices was selected (Valkonen 2011). The cumulative basal area distributions of the trees were divided into three classes of equal size, and two sample trees were randomly sampled from each class. 12 trees were sampled. Detailed experimental design and stand descriptions are given in Piispanen et al. (2014).

2.3. Measurement of tracheid width

Disks were sawn at a height of 0.6 m and 1 m from each UAS and EAS tree respectively. Radial sample bars with cross-sections approximately 1 cm x 1 cm were sawn from the pith to the bark along the northern radius. The bars were air-dried, after which a radial sample strip (2 mm tangentially and 7 mm longitudinally) was sawn from each bar. They were extracted with acetone in a Soxhlet Extractor at 56.2 ^{o}C for 6 h, and their upper surfaces were finely polished. They were stored in the conditioned measurement laboratory for even moisture content before characterization of the radial variations in several tracheid and wood properties from pith to bark with the SilviScan instrument (Innventia Ab, Stockholm, Sweden) (Evans *et al.* 1995). SilviScan integrates three measurement principles: image analysis of tracheid cross-sections; X-ray absorption to measure wood density; and X-ray diffraction to measure the microfibril angle of wood strips (Evans 1994; Evans and Elic 2001). In this study, image analysis and X-ray absorption were used for measuring tracheid width, widths in the radial and tangential directions, in radial intervals of 25 µm (Piispanen et al. 2014).

The locations of all annual rings and the interfaces between their parts of earlywood, transition wood, and latewood were determined from the radial variations in wood density (Lundqvist et al. 2018). The ring boundaries were determined using an algorithm that detected the steep density decrease that occurs between the latewood and the earlywood. As many annual rings in UAS trees were exceptionally narrow, cross-checking was conducted to assure the locations of annual ring boundaries optically on samples taken perpendicular to those for the SilviScan measurements (Piispanen *et al*. 2014). The same samples were remeasured using a computer-aided system consisting of an Olympus SZ51 stereo microscope (Olympus corporation,

Tokyo, Japan) connected to a Heidenhein LS 303C transducer (Encoders UK Ltd. Birmingham, UK) with an accuracy of 0.001 mm (Piispanen et al. 2014).

After the setting of ring boundaries and the cross-checking, a "20–80" density threshold definition was applied for separating three compartments within each ring. The span from minimum to maximum wood density was determined based on the SilviScan measurements: The part from 0 to 20% of the span was classified as earlywood, the part from 80 to 100% as latewood, and the part between as transition wood (Lundqvist et al. 2018).

From the locations, ring distance from pith (stem radius, *R*), ring number from the pith (cambial age, *CA*), ring widths (*RW*), latewood and transitionwood widths and proportions (*LWW, TWW*, *LWP* and *TWP*, respectively) were calculated. Arithmetic means of radial tracheid widths was calculated for each ring (*Width*), as well as for its earlywood (*WidthEW*), latewood (*WidthLW*) and transitionwood (*WidthTW*). A total of 6004 and 1191 annual rings in the UAS and EAS trees were measured, respectively.

The first five rings were excluded as the innermost rings are too curved to allow precise data acquisition for each ring and its parts with the x-ray beam passing through the 2 mm thick sample strip.

2.4. Measurement of tracheid length

Disks were sawn just below a height of 0.6 m and 1.0 m from each UAS and EAS tree respectively. In UAS, only trees from sites LAP and VES were included. A radial strip (0.5 cm tangentially and 1.5 cm longitudinally) was sawn from the pith to the bark along the north radius from each disk. For UAS trees, one-centimeter-long radial samples were cut from the 0.5-cm-wide strip from pith to cambium and cut into

match-size sticks for maceration. For UAS trees, the *R* and *CA* of the samples refer to the values of the rings of the oldest cambial age of the 1-cm section of the radial samples, and *RW*, *LWW*, and *TWW* were defined as sample-specific averages. For EAS trees, earlywood samples were taken from selected single annual rings and cut into match-size sticks for maceration. After analysis, the means of the tracheid lengths in the EW samples were calculated. In EAS trees, R and CA referred to the exact rings. A total of 754 and 30 samples with 50 tracheids each was gained for UAS and EAS trees respectively.

Prior to the analyses of tracheid length, the samples were macerated in glacial acetic acid/30% hydrogen peroxide (1:1, v/v) overnight at 60 °C. The resulting suspension of the liberated washed fibers of each sample was applied to four microscope slides. Fifty unbroken tracheids per sample were measured with an Olympus BH-2 microscope (Olympus Optical, Tokyo, Japan) and a CCDC Camera (COHU MOD 4912-5000/0000, Cohu, San Diego, CA) in conjunction with the Image-Pro Plus 3.0 program for Windows (Media Cybernetics, Silver Spring, MD). One pixel corresponded to 1.08 µm. The mean of the tracheid lengths measured was used to describe the tracheid length (*L*).

2.5. Statistical analysis

We analyzed the variation of tracheid *Width* and *Length* in UAS and EAS, using modeling as the primary statistical approach. Linear mixed modeling was applied to account for the random variances arising from the hierarchical structure of the data (Dutilleul et al. 1998; Downes et al. 2002). Variance components (VC) for plot, tree, and growth ring levels were incorporated in the mixed models to allow individual

observations to vary around the population, plot, and tree means respectively. First-order autoregression (AR(1)) was applied to adjacent rings, as they are often correlated (Dutilleul et al. 1998; Downes et al. 2002).

The data from the first five annual rings were excluded from both modeling datasets, according to the limitations in measuring the narrow rings near the pith (see above). Upon screening the linear mixed model candidates, we found that one tree had exceptionally small tracheids, probably due to a very high compression wood content, and that tree was excluded from the modeling data. The eventual number of samples used for modeling *Width* and *Length* was then 5598 and 709 respectively.

Because our response variables were mean values of entire growth rings (or several rings in the case of *Length* of UAS trees), they were modeled with respect to ring-level attributes: *R*, *CA*, *RW*, and the widths and proportions of LW and TW (*LWW*, *TWW*, *LWP*, and *TWP*).

The growth trends of cell dimensions in the radial direction are well established - several studies have used e.g. logarithmic or exponential functions to describe the pith-to-bark developments (Lundqvist et al. 2005; Franceschini et al. 2012; Piispanen et al. 2014). In this study, we used logarithmic transformations of the response variables, and *R* and *CA* were the first to be tested in models for both dimensions. Subsequently, *RW* and its various transformations were tested in the models, with the assumption that they could explain additional variance along the radial trend caused by differences in growth conditions, tree position, and other factors affecting *RW*. In addition, *LWP* (and *TWP*, to a lesser extent) is known to be an important explanatory variable for the ring-specific means of tracheid dimensions, due to LW tracheid properties that differ from those in EW (Lindström 1997). It has also been argued that

283 *LWP* (often negatively correlated with *RW*) could actually express most of the
284 variance often attributed to *RW* (Downes et al. 2002). We therefore also tested *LWP*
285 and *TWP* in our models.

286 Relative stem size (dbh/dbh_{dom}), where *dbh* is the individual tree stem diameter at
287 breast height and dbh_{Dom} is the average stem diameter of the 100 thickest trees ha^{-1})
288 was tested as a fixed variable explaining tree-specific variations of tracheid
289 dimensions. *Site* was tested as a fixed variable to account for the differences between
290 the studied sites that were not captured by the selected explanatory variables.

291 Following the screening of various combinations of the explanatory variables and
292 their transformations and mutual correlations (Tables *A1* and *A2* in Supplementary
293 material), final models were selected based on visual inspections. Model fit and
294 unbiasedness were ensured by the visual examination of model residuals with respect
295 to the observed values, as well as the explanatory variables, and the statistical
296 significance of the parameter estimates. The predicted response variable values ln ($\hat{y}$)
297 were retransformed to the original scale (µm and mm for *Width* and *Length*
298 respectively) using the following equation:

299 $$\hat{y} = e^{\widehat{\ln(y)} + (\delta_{k_j} + \alpha_j)/2} \quad (1),$$

300 where δ_{kj} and α_j are the random terms for tree- and plot-level effects, respectively. The
301 correction term was added to the estimates of the intercepts.

302

303 Differences of tracheid dimensions between EAS and UAS were examined by
304 applying the UAS models (2 and 3) to the data for EAS and analyzing the errors.

305 All statistical analyses were carried out using SPSS© version 25 (IBM 2018).

3. Results

3.1. Empirical results

Both tracheid dimensions increased logarithmically with greater *R* and *CA* (Figures 2, 3). In UAS, differences in the tracheid dimensions between the size classes of trees were notable with respect to *CA*, while the differences were less pronounced with respect to *R*.

Tracheid *Width* showed a larger range of variation in UAS trees of different sizes than in EAS trees, in general and when related to *R, CA*, *RW,* and *LWP* (Figure 2, Table 2). A major difference between the two treatments was observed for the innermost 10 annual rings, where the UAS trees had a much steeper increase in the tracheid widths, synchronous to the rapid decrease in *LWP* (Figure 1).

In UAS, tracheid *Length* was largely independent of *RW*. However it differed among the size classes (Figure 3, Table 2), and had a negative correlation with *LWP*.

3.2. Tracheid dimension models

The finally selected tracheid dimension models were:

$$\ln Width_{ijkl} = b_0 + b_1 * Site_i + b_2 * \ln R_{ijkl} + b_3 * CA^2{}_{ijkl} + b_4 * RW_{ijkl} + b_5 * RW^2{}_{ijkl} + b_6 * \ln LWP_{ijkl} + b_7 * lnTWP_{ijkl} + \varepsilon_{ij} + \varepsilon_{ijk} + \varepsilon_{yearl} + \varepsilon_{ijkl} \quad (2)$$

$$\ln Length_{ijkm} = b_0 + b_1 * Site_i + b_2 * \ln R_{ijkm} + b_3 * lnCA_{ijkm} + b_4 * CA^2{}_{ijkm} + b_5 * RW_{ijkm} + b_6 * \ln LWP_{ijkm} + b_7 * lnTWP_{ijkm} + \varepsilon_{ij} + \varepsilon_{ijk} + \varepsilon_{yearm} + \varepsilon_{ijkm} \quad (3)$$

Readers are referred to the parameter definitions in Table 1, except:

i, j, k, l, m = Indicators of hierarchy in the data: annual ring *l* in tree *k* on plot *j* at site *i*; in model 3 for *L*, R_{ijkm} and CA_{ijkm} represent the edge furthest from the pith of the 1-cm thick sample *m* in tree *k* on plot *j* at site *i*, and other fixed variables in model 3 are averages in the 1-cm thick sample;

ε_{ij} = Random effect of plot within site

ε_{ijk} = Random effect of tree on plot within site

ε_{yearl} or ε_{yearm} = Random effect of calendar year (when the annual ring was established), also including an autocorrelation parameter ρ_{ijkl} with the AR(1) structure between successive calendar years

ε_{ijkl} or ε_{ijkm} = Residual.

In total, the models explained 92.4% and 84.2% of the variance of *Width* and *Length* in UAS data respectively. We found *R* and *RW* the most important predictors of *Width* (Table 3), while *Length* was mostly explained by *R* and *CA* (Table 4). The combined effects of the independent variables *CA*, *RW*, and *LWP* on *Width* and *Length* in trees under UAS management were simulated across relevant ranges and are illustrated in Figure 4.

In general, our model (Equation 2) predicted increasing *Width* for UAS trees with ageing cambium, increasing *RW*, and decreasing *LWP* (Table 3). More specifically, the effects of *RW* and *LWP* were limited during the juvenile phase ($CA < 20$) but became increasingly influential as the cambium aged (Figure 4). The most distinct enlargement of *Width* was predicted with $CA > 60$ a, $RW > 4$ mm and $LWP < 10$ (Figure 4).

According to the model (Equation 3), *Length* increased with *CA* and showed a negligible decrease with increasing *RW* and *LWP*, most pronouncedly at ages between 30 and 50 (Table 4), after which the influence of CA fully dominated (Figure 4).

3.3. Comparison between UAS and EAS

The application of the models (Equations 2 and 3) to EAS data—i.e. predictions of tracheid dimensions in EAS trees using the parameter estimates fitted to UAS data (Tables 3 and 4)—resulted in notable prediction errors in *Width* and *Length*. Smaller values were underestimated and larger values overestimated, and the overestimation increased toward the stem surface (Figure 5). These errors reflected the smaller range of *Width* values in the EAS data (Figure 2), but also the trend of increasing *RW* synchronously to decreasing *LWP* towards stem surface (Figure 1) that was associated with increasing *Width* in the UAS data but was absent in the EAS data (Figure 5). The similar prediction errors of *Length* were slightly affected by the differences in the growth rates between EAS and UAS (Figure 5).

4. Discussion

Tracheid length and width patterns from pith to bark in uneven-aged Norway spruce (*Picea abies* L. (H.) Karst) trees were addressed. The identification of main factors and a comparison with even-aged stands were also pursued.

The wood samples were taken near the stem base (0.6 m) to cover the full range of the annual ring width patterns in uneven-aged stands. However, the study material cannot be considered representative of tracheid properties at other heights along the stem. The difference in sampling heights (1.0 m for EAS vs. 0.6 m for UAS) should not have had a major influence on the results The sample size for tracheid length for EAS (30 samples, 1500 tracheids) is not large enough to yield valuable insight into the patterns beyond general trends.

We observed patterns of tracheid dimensions developments that reflected the effects of the initial suppression in the early years, and the gradual release toward the dominant phase. In the UAS material, the latewood proportions in the innermost rings were at relatively high levels (~30%), followed by a steep decrease. Correspondingly rapid increases in the tracheid dimensions in the corewood of the UAS trees were also observed. On the other hand, low latewood percentages and large ring widths were observed in the UAS outerwood, where the tracheids were wider and longer.

Both cambial age and stem radius were included in the final models despite their obvious autocorrelation, as their counteraction reflected the effects of shifting canopy positions characteristic of trees grown under the UAS regime. The intra-annual variations of tracheid dimensions due to differing compositions of early-, transition-, and latewood were accounted for in our models by including ring width, latewood, and earlywood proportion in the fixed parts. Their application in the model estimation and application also accounted for the different sampling designs used in the UAS and EAS study materials: tracheid length for UAS trees was measured from 1-cm radial samples entailing entire growth rings including early-, transition-, and latewood proportions, while that of EAS was measured from pure earlywood samples.

In our models, ring width had more pronounced positive effects onto tracheid widths in the outerwood than in the corewood, and showed only negligible, negative effects on tracheid lengths in addition to the dominant effects of cambial age and stem radius. It is noteworthy that total tree age has been found to be positively correlated with the rate of cell division (Rathgeber et al. 2011; Lundqvist et al. 2018), which is a main determinant of ring width. Subsequently, the observed positive effects of ring width on tracheid width could also be corollary to increasing tree age and stem radius, rather than causal *per se*.

Based on our data and literature, corewood in EAS trees exhibits large ring widths with high earlywood contents, and the proportion of corewood in stems is high (Downes et al. 2002; Sarén et al. 2004; Lundqvist et al. 2005; Lasserre et al. 2009). However, we observed contrasting trends in the UAS trees. The differences may be related to the maturation processes in cambium due to the long period of slow growth resulting from the suppression phase typical in UAS. Most UAS trees in our data had thinner rings and higher latewood proportion in their corewood, as opposed to the wider rings with a higher earlywood proportion in the EAS corewood. At a similar stem radius, the cambium in UAS was thus generally older than in EAS (i.e. had higher cambial age). Tracheids from dominant UAS trees (DBH≥30 cm; wider rings and lower latewood proportion) reached larger dimensions at smaller stem radius and younger cambial age compared to EAS. The outerwood in dominant UAS trees had wider tracheids than those in EAS. In contrast, tracheids from the outerwood of suppressed UAS trees (DBH<10 cm; thinner rings and higher latewood proportion), remained narrower than their EAS counterparts.

Despite the differences, our results concur with similar observations about the age- and size-mediation of tracheid dimension maturation in the major body of the

previous literature, e.g. Lindström (1997); Mäkinen *et al.* (2007); Franceschini et al. (2012) and Sirviö and Kärenlampi (2001). The predominant relationships of tracheid dimensions with cambial age and stem radius reflect the structural-functional relationship of tracheid dimensions with turgor pressure and hydraulic resistance in water transport, which change as the tree ages and grows in height and crown size (Mansfield et al. (2007), Kuprevicius et al. (2013), Sorce et al. 2013). Large UAS Norway spruces may maintain long vigorous crowns when in dominant positions (Kumpu et al. 2020), and produce wood with high earlywood content and wide tracheids at the base of the stem to sustain the water conductivity.

In a study of the wood properties of black spruce (*Picea mariana* (Mill.) in even- and uneven-aged boreal stands in Eastern Canada, Pamerleau-Couture et al. (2019) concluded that most measured wood properties were correlated with ring width, and there were major differences between even-aged and uneven-aged stands submitted to partial cutting. Ring width, tracheid length, latewood and maximum wood density were higher in the even-aged trees than in the uneven-aged trees. These findings diverge partly from those of this study and those of Piispanen et al. (2014) on wood density in our experimental stands. However, direct comparisons are not very meaningful due to the large differences between the materials (geographical location, tree species, intensity and type of cuttings, time elapsed after cuttings).

In conclusion, the development of tracheid dimensions between UAS and EAS trees follows similar age and size-dependent relationships. However, the extended suppression phase in the early growth of UAS trees tends to increase the proportion of wider and longer tracheids at the base of the stem. Moreover, old UAS trees in dominant positions produce wood with a high earlywood content. The results suggest that extending the growth of mature trees before harvesting increases the recovery of

wood with properties well-suited for most end uses. In UAS, the conditions for prolonging the lifespan of trees may be superior to those in EAS, due to the increased ring widths (as a proxy for growth rate) in the wood of the dominant UAS trees. Our results mainly apply to the lower parts of trees, which constitute the main product of UAS as valuable sawlogs. The outermost parts are often used in pulping, for which their fiber properties seem very good.

Acknowledgements

We gratefully acknowledge the technical skills of Pekka Helminen, Tapio Järvinen, Juhani Korhonen, Tapio Nevalainen, and Hilkka Ollikainen (Natural Resources Institute Finland) and Thomas Grahn, Åke Hansson, and Lars Olsson (RISE Innventia AB, Sweden). Södra Cell is acknowledged for wood material from Swedish Norway spruce even-aged sites. The EAS data reused for this study had originally been created in terms of the project “Multi-sectorial database, model system and case studies, supporting innovative use of wood and fibres” (Innovood), which belonged to the Wood Material Science and Engineering Finnish–Swedish Research Program, which had been funded by BUSINESS FINLAND (formerly Tekes) and VINNOVA on the Swedish side. We thank Harri Mäkinen for kindly providing the EAS tracheid length data.

Competing interests statement

The authors declare there are no competing interests.

References

467 Ahlström, M.A., and Lundqvist, L. 2015. Stand development during 16–57 years in partially
468 harvested sub-alpine uneven-aged Norway spruce stands reconstructed from
469 increment cores. For. Ecol. Manage. **350**, 81-86. doi:10.1016/j.foreco.2015.04.021.
470 Assmuth, A., and Tahvonen, O. 2018. Optimal carbon storage in even-and uneven-aged
471 forestry. For. Policy Econ. **87**, 93-100. doi:10.1016/j.forpol.2017.09.004.
472 Boucher, Y., Perrault-Hébert, M., Fournier, R., Drapeau, P., and Auger, I. 2017. Cumulative
473 patterns of logging and fire (1940–2009): consequences on the structure of the eastern
474 Canadian boreal forest. Landscape Ecol. **32** (2), 361-375. doi:10.1007/s10980-016-
475 0448-9.
476 Cajander, A.K. 1949. Forest types and their significance. Acta For. Fenn. **56** (4), 1-69.
477 Downes, G.M., Wimmer, R., and Evans, R. 2002. Understanding wood formation: gains to
478 commercial forestry through tree-ring research. Dendrochronol. **20** (1-2), 37-51.
479 doi:10.1078/1125-7865-00006.
480 Dutilleul, P., Herman, M., and Avella-Shaw, T. 1998. Growth rate effects on correlations
481 among ring width, wood density, and mean tracheid length in Norway spruce (Picea
482 abies). Can. J. For. Res. **28** (1), 56-68.
483 Eerikäinen, K., Valkonen, S., and Saksa, T. 2014. Ingrowth, survival and height growth of
484 small trees in uneven-aged Picea abies stands in southern Finland. For. Ecosys. **1** (1),
485 5. doi:10.1186/2197-5620-1-5.
486 Evans, R. 1994. Rapid measurement of the transverse dimensions of tracheids in radial wood
487 sections from Pinus radiata. Holzforsch. **48** (2), 168-172.
488 doi:10.1515/hfsg.1994.48.2.168.
489 Evans, R., Downes, G., Menz, D., and Stringer, S. 1995. Rapid measurement of variation in
490 tracheid transverse dimensions in a radiata pine tree. Appita J. **48** (2), 134-138.
491 https://search.informit.org/doi/epdf/10.3316/informit.252935342865527.

492 Evans, R., and Elic, J. 2001. Rapid prediction of wood stiffness from microfibril angle and
493 density. For. Prod. J. **51** (3), 53-57.
494 Fabris, S. 2000. Influence of cambial ageing, initial spacing, stem taper and growth rate on
495 the wood quality of three coastal conifers. Ph.D. Thesis. University of British
496 Columbia. Canada. doi: 10.14288/1.0089742.
497 Franceschini, T., Lundqvist, S.-O., Bontemps, J.-D., Grahn, T., Olsson, L., Evans, R., and
498 Leban, J-M. 2012. Empirical models for radial and tangential fibre width in tree rings
499 of Norway spruce in north-western Europe. Holzforsch. **66** (2), 219-230.
500 doi:10.1515/HF.2011.150.
501 García-Tejero, S., Spence, J.R., O'Halloran, J., Bourassa, S., and Oxbrough, A. 2018. Natural
502 succession and clearcutting as drivers of environmental heterogeneity and beta
503 diversity in North American boreal forests. PloS ONE, **13** (11), e0206931. |
504 doi:10.1371/journal.pone.0206931.
505 Gauthier, S., Bernier, P., Kuuluvainen, T., Shvidenko, A., and Schepaschenko, D. 2015.
506 Boreal forest health and global change. Sci. **349** (6250), 819-822.
507 doi:10.1126/science.aaa9092.
508 Hynynen, J., Eerikäinen, K., Mäkinen, H., and Valkonen, S. 2019. Growth response to
509 cuttings in Norway spruce stands under even-aged and uneven-aged management.
510 For. Ecol. Manage. **437**, 314-323. doi:10.1016/j.foreco.2018.12.032.
511 Kumpu, A., Piispanen, R., Berninger, F., Saarinen, J., and Mäkelä, A. 2020. Biomass and
512 structure of Norway spruce trees grown in uneven-aged stands in southern Finland.
513 Scan. J. For. Res. **35**, 252-261. doi:10.1080/02827581.2020.1788138.
514 Kuprevicius, A., Auty, D., Achim, A., and Caspersen, J.P. 2013. Quantifying the influence of
515 live crown ratio on the mechanical properties of clear wood. For. **86** (3), 361-369.
516 doi:10.1093/forestry/cpt006.

517 Laamanen, V. 2014. Structure of selection cutting stands, logging conditions, logging costs
518 and logging damages. Master's thesis, University of Helsinki. 85 + 5 p. In Finnish
519 with English abstract.
520 Lasserre, J.-P., Mason, E.G., Watt, M.S., and Moore, J.R. 2009. Influence of initial planting
521 spacing and genotype on microfibril angle, wood density, fibre properties and
522 modulus of elasticity in Pinus radiata D. Don corewood. For. Ecol. Manage. **258** (9),
523 1924-1931. doi:10.1016/j.foreco.2009.07.028.
524 Lindström, H. 1997 Fiber length, tracheid diameter, and latewood percentage in Norway
525 spruce: development from pith outward. Wood Fiber Sci. **29** (1), 21-34.
526 https://wfs.swst.org/index.php/wfs/article/view/2081
527 Lundqvist, S.-O., Grahn, T., Hedenberg, Ö. 2005. Models for fibre dimensions in different
528 softwood species. Simulation and comparison of within and between tree variations
529 for Norway and Sitka spruce, Scots and Loblolly pine. In: 5th workshop on "Wood
530 quality modelling", IUFRO Working Party 5.01.04, Auckland, New Zealand, Nov
531 22–27 2005.
532 Lundqvist, S.-O., Seifert, S., Grahn, T., Olsson, L., García-Gil, M.R., Karlsson, B., and
533 Seifert, T. 2018. Age and weather effects on between and within ring variations of
534 number, width and coarseness of tracheids and radial growth of young Norway
535 spruce. Eur. J. For. Res. **137** (5), 719-743. doi:10.1007/s10342-018-1136-x.
536 Macdonald, E., Gardiner, B., and Mason, W. 2010. The effects of transformation of even-
537 aged stands to continuous cover forestry on conifer log quality and wood properties in
538 the UK. Forestry, **83** (1), 1-16. doi:10.1093/forestry/cpp023.
539 Mäkinen, H., Jaakkola, T., Piispanen, R., and Saranpää, P. 2007. Predicting wood and
540 tracheid properties of Norway spruce. For. Ecol. Manage. **241** (1), 175-188.
541 doi:10.1016/j.foreco.2007.01.017.

542 Mansfield, S.D., Parish, R., Goudie, J.W., Kang, K.-Y., and Ott, P. 2007. The effects of
543 crown ratio on the transition from juvenile to mature wood production in lodgepole
544 pine in western Canada. Can. J. For. Res. **37** (8), 1450-1459. doi:10.1139/X06-299.
545 Natural Resources Institute Finland. 2018. Statistics database, https://stat.luke.fi/en/uusi-
546 etusivu.
547 Nolet, P., Kneeshaw, D., Messier, C., and Béland, M. 2018. Comparing the effects of
548 even-and uneven-aged silviculture on ecological diversity and processes: A review.
549 Ecol. Evol. **8** (2), 1217-1226. doi:10.1002/ece3.3737.
550 Pamerleau-Couture, É., Rossi, S., Pothier, D., and Krause, C. 2019. Wood properties of black
551 spruce (Picea mariana (Mill.) BSP) in relation to ring width and tree height in even-
552 and uneven-aged boreal stands. Ann. For. Sci. **76** (2), 43. doi:10.1007/s13595-019-
553 0828-9.
554 Piispanen, R., Heinonen, J., Valkonen, S., Mäkinen, H., Lundqvist, S.-O., and Saranpää, P.
555 2014. Wood density of Norway spruce in uneven-aged stands. Can. J. For. Res. **44**
556 (2), 136-144. doi:10.1139/cjfr-2013-0201.
557 Piispanen, R., Heikkinen, J., and Valkonen, S. 2020. Deformations of boards from uneven-
558 aged Norway spruce stands. Eur. J. Wood Wood Prod. **78**, 533-544.
559 doi:10.1007/s00107-020-01524-x.
560 Pretzsch, H. and Rais, A. 2016. Wood quality in complex forests versus even-aged
561 monocultures: review and perspectives. Wood Sci. Technol. **50** (4), 845-880.
562 doi:10.1007/s00226-016-0827-z.
563 Puettmann, K.J., Wilson, S.McG., Baker, S.C., Donoso, P.J., Drössler, L., Amente, G.,
564 Harvey, B.D., Knoke, T., Lu, Y., Nocentini, S., Putz, F.E., Yoshida, T., and Bauhus,
565 J. 2015. Silvicultural alternatives to conventional even-aged forest management-what
566 limits global adoption? For. Ecosyst. **2** (1), 8. doi:10.1186/s40663-015-0031-x.

567 Rantala, S. 2011. Finnish forestry practice and management. Metsäkustannus, Helsinki,
568 Finland. 271 p.
569 Rathgeber, C.B.K., Rossi, S., and Bontemps, J.-D. 2011. Cambial activity related to tree size
570 in a mature silver-fir plantation. Ann. Bot. **108** (3), 429-438. doi:10.1093/aob/mcr168.
571 Saksa, T., and Valkonen, S. 2011. Dynamics of seedling establishment and survival in
572 uneven-aged boreal forests. *For. Ecol. Manage.* **261** (8), 1409-1414.
573 doi:10.1016/j.foreco.2011.01.026.
574 Sarén, M.-P., Serimaa, R., Andersson, S., Saranpää, P., Keckes, J., and Fratzl, P. 2004. Effect
575 of growth rate on mean microfibril angle and cross-sectional shape of tracheids of
576 Norway spruce. Trees, **18** (3), 354-362. doi:10.1007/s00468-003-0313-8.
577 Savva, Y., Koubaa, A., Tremblay, F., and Bergeron, Y. 2010. Effects of radial growth, tree
578 age, climate, and seed origin on wood density of diverse jack pine populations. Trees,
579 **24**, 53–65. doi: 10.1007/s00468-009-0378-0.
580 Schrader, J., Baba, K., May, S., Palme, K., Bennett, M., Bhalerao, R., and Sandberg, G. 2003.
581 Polar auxin transport in the wood-forming tissues of hybrid aspen is under
582 simultaneous control of developmental and environmental signals. PNAS, **100** (17),
583 10096-10101. doi:10.1073/pnas.1633693100.
584 Schütz, J.-P. 2001. Opportunities and strategies of transforming regular forests to irregular
585 forests. For. Ecol. Manage. **151** (1-3), 87-94. doi:10.1016/S0378-1127(00)00699-X.
586 Seeling, U. 2001. Transformation of plantation forests – expected wood properties of Norway
587 spruce (*Picea abies* (L.) Karst.) within the period of stand stabilisation. For. Ecol.
588 Manage. 151(1-3): 195-210. doi:10.1016/S0378-1127(00)00708-8.
589 Sirviö, J., and Kärenlampi, P. 2001. The effects of maturity and growth rate on the properties
590 of spruce wood tracheids. Wood Sci. Technol. **35** (6), 541-554.
591 doi:10.1007/s002260100119.

592 Sorce, C., Giovannelli, A., Sebastiani, L., and Anfodillo, T. 2013. Hormonal signals involved
593 in the regulation of cambial activity, xylogenesis and vessel patterning in trees. Plant
594 Cell Rep. **32** (6), 885-898. doi:10.1007/s00299-013-1431-4.
595 Valkonen, S. 2011 Tree species. *In* Finnish Forestry-Practice and Management. *Edited by* S.
596 Rantala. Metsäkustannus, Helsinki, Finland. pp. 35-36.
597 Zobel, B.J., and Jett, J.B. 1995. Genetics of wood production. *In* Springe Series of Wood
598 Science. 1st ed. Springer-Verlag Berlin Heidelberg, Germany. 337 p.
599

600
601 **Table 1.** List of variables, their abbreviations, explanations, and units.

602 **Table 2.** Averages, standard deviations and minimum and maximum values for radial
603 tracheid width and tracheid length by tree size classes.

604 **Table 3.** Parameter coefficient estimates for the linear mixed model of radial tracheid
605 width (Eq. 2), and standard errors (SE) and statistical significances (p). For
606 abbreviations see Table 1.

607 **Table 4.** Parameter coefficient estimates for the linear mixed model of tracheid length
608 (Eq. 3), and the standard errors (SE) and statistical significances (p). For
609 abbreviations see Table 1.

610 **Table A1.** Pearson correlation coefficients (r) and significance levels (*p*) between key
611 variables in the data used for modeling tracheid width.

612 **Table A2.** Pearson correlation coefficients (r) and significance levels (*p*) between key
613 variables in the data used for modeling tracheid length.

614

615

616 Figure captions

617 Figure 1. Observed ring widths and latewood and transition wood percentages in
618 uneven-aged and even-aged stands (UAS and EAS) with respect to cambial age in the
619 four size classes. Lines indicate class means at 15 equal intervals with respect to the
620 x-axis. The data correspond to those used in the measurement of the tracheid widths:
621 for UAS and EAS n = 6004 and n = 1191 respectively.

622 Figure 2. Observed tracheid widths in uneven-aged and even-aged stands (UAS and
623 EAS) with respect to stem radius, cambial age, ring width and latewood percentage in
624 the four size classes. Lines indicate class means at 15 equal intervals with respect to
625 the x-axis. For UAS and EAS, n = 6004 and n = 1191, respectively.

626 Figure 3. Observed tracheid lengths in uneven-aged and even-aged stands (UAS and
627 EAS) with respect to stem radius, cambial age, ring width and latewood percentage in
628 the four size classes. Lines indicate class means at 15 equal intervals with respect to
629 the x-axis. For UAS and EAS n = 754 and n = 30, respectively.

630 Figure 4. Predicted tracheid widths and predicted tracheid lengths in UAS trees with
631 respect to cambial age, ring width and latewood percentage, using the models fitted to
632 data from the UAS trees. The colors indicate the width (upper panes) and length
633 (lower panes) of the tracheids with respect to the combined effects of cambial age (x-
634 axis), and ring width, or latewood percentage (y-axis).

635 Figure 5. Prediction errors of the tracheid dimensions in even-aged stands (EAS),
636 when EAS data are used as inputs to the models fitted to uneven-aged data. The
637 prediction errors are given with respect to the predicted values and the fixed variables
638 stem radius, ring width, and latewood percentages in EAS.

Table 1. List of main variables studied in this study, their abbreviations, explanations and units.

Abbreviation	Explanation	Unit
Width	Radial tracheid width	μm
WidthLW	Radial tracheid width in latewood	μm
WidthEW	Radial tracheid width in earlywood	μm
WidthTW	Radial tracheid width in transitionwood	μm
Length	Tracheid length	mm
R	Stem radius at the position of a specific sampling point,	mm
CA	Cambial age	a
RW	Annual ring width	mm
EWW	Earlywood width	mm
LWW	Latewood width	mm
TWW	Transitionwood width	mm
LWP	Latewood percentage	%
TWP	Transitionwood percentage	%
dbh	Diameter-at-breast-height	mm
dbh_{dom}	Mean d of 100 largest trees per hectare	mm
Site	The locality of studied stand (as below)	dummy
- LAP	Lapinjärvi	
- VES	Vesijako	
- SUO	Suonenjoki	

Table 2. Averages, standard deviations and minimum and maximum values for radial tracheid width and tracheid length by tree size classes.

Radial tracheid width (μm)								
	UAS				EAS			
Size class (cm)	mean	sd	min	max	mean	sd	min	max
0 – 9.99	24.84	3.15	15.42	33.10	29.63	1.70	24.90	32.83
10 – 19.99	27.58	3.47	17.59	35.79	30.67	1.87	25.63	35.95
20 – 29.99	29.21	3.89	17.10	38.26	30.54	1.65	23.49	34.75
30 –	31.67	3.85	18.92	40.43	30.48	1.89	24.45	35.94
Tracheid length (mm)								
	UAS				EAS			
Size class	mean	sd	min	max	mean	sd	min	max
0 – 9.99	2.41	0.54	1.08	3.32	NA	NA	NA	NA
10 – 19.99	2.65	0.61	1.15	3.80	NA	NA	NA	NA
20 – 29.99	2.80	0.62	1.15	4.23	3.44	0.67	2.18	4.55
30 –	3.04	0.61	1.02	4.20	3.21	0.59	2.19	3.95

Table 3. Parameter estimates for the model of radial tracheid width (Eq. 2), and the standard errors (SE) and statistical significances (p). For abbreviations see Table 1.

Parameter	Estimate	SE	p
Fixed effects			
Intercept, b_0	3.0390	0.0158	<0.01
$Site_i$, b_1			
LAP	-0.0710	0.0123	<0.01
VES	0.0033	0.0112	0.77
SUO	0.0000	0.0000	.
$\ln R_{ijk}$, b_2	0.1194	0.0019	<0.01
CA^2_{ijkl}, b_3	-0.00000177	0.000000883	0.05
RW_{ijkl}, b_4	0.0487	0.0027	<0.01
RW^2_{ijkl}, b_5	-0.0053	0.0005	<0.01
$\ln LWP_{ijkl}$, b_6	-0.0331	0.0012	<0.01
$\ln TWP_{ijkl}$, b_7	-0.0253	0.0014	<0.01
Random effects			
Plot, σ^2_{ij}	0.0001	0.0001	0.61
Tree, σ^2_{ijk}	0.0017	0.0003	<0.01

Year, σ^2_{yearl}	0.0002	0.0000	<0.01
Year AR(1), ρ	0.5019	0.0139	<0.01
Residual, σ^2_{ijkl}	0.0017	0.0000	<0.01

Table 4. Parameter estimates for the model of tracheid length (Eq. 3), and the standard errors (SE) and statistical significances (p). For abbreviations see Table 1.

Parameter	Estimate	SE	p
Fixed effects			
Intercept, b_0	-0.0824	0.0600	0.14
Site$_i$, b_1			
LAP	-0.1747	0.0263	<0.01
VES	0.0000	0.0000	.
lnR_{ijk}, b_2	0.2016	0.0210	<0.01
$lnCA_{ijkl}$, b_3	0.1698	0.0278	<0.01
CA^2_{ijkl}, b_4	-0.00003060785	0.000005165204	<0.01
RW_{ijkl}, b_5	-0.0184	0.0045	<0.01
ln LWP_{ijkl}, b_6	-0.0156	0.0071	0.03
ln TWP_{ijkl}, b_7	-0.0212	0.0099	0.03
Random effects			
Plot, σ^2_{ij}	0.0004	0.0007	0.59
Tree, σ^2_{ijk}	0.0026	0.0017	0.13
Year, σ^2_{yearl}	0.0001	0.0001	0.34

Year AR(1), ρ	0.9353	0.0133	<0.01
Residual, σ^2_{ijkl}	0.0012	0.0020	<0.01

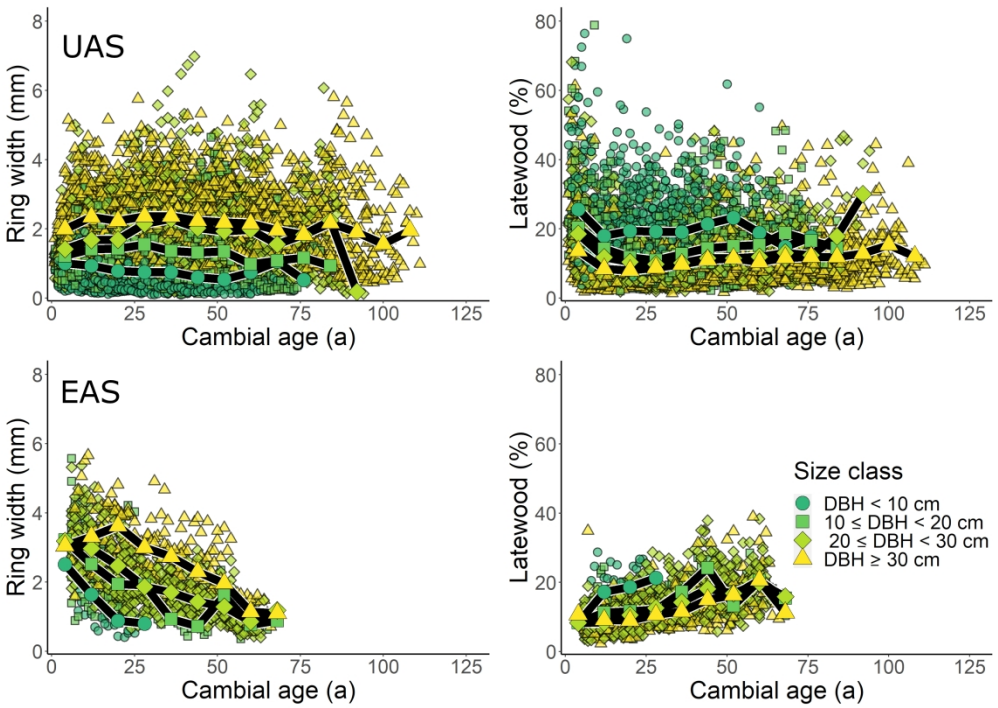

Figure 1. Observed ring widths and latewood and transition wood percentages in uneven-aged and even-aged stands (UAS and EAS) with respect to cambial age in the four size classes. Lines indicate class means at 15 equal intervals with respect to the x-axis. The data correspond to those used in the measurement of the tracheid widths: for UAS and EAS n = 6004 and n = 1191 respectively.

1089x769mm (96 x 96 DPI)

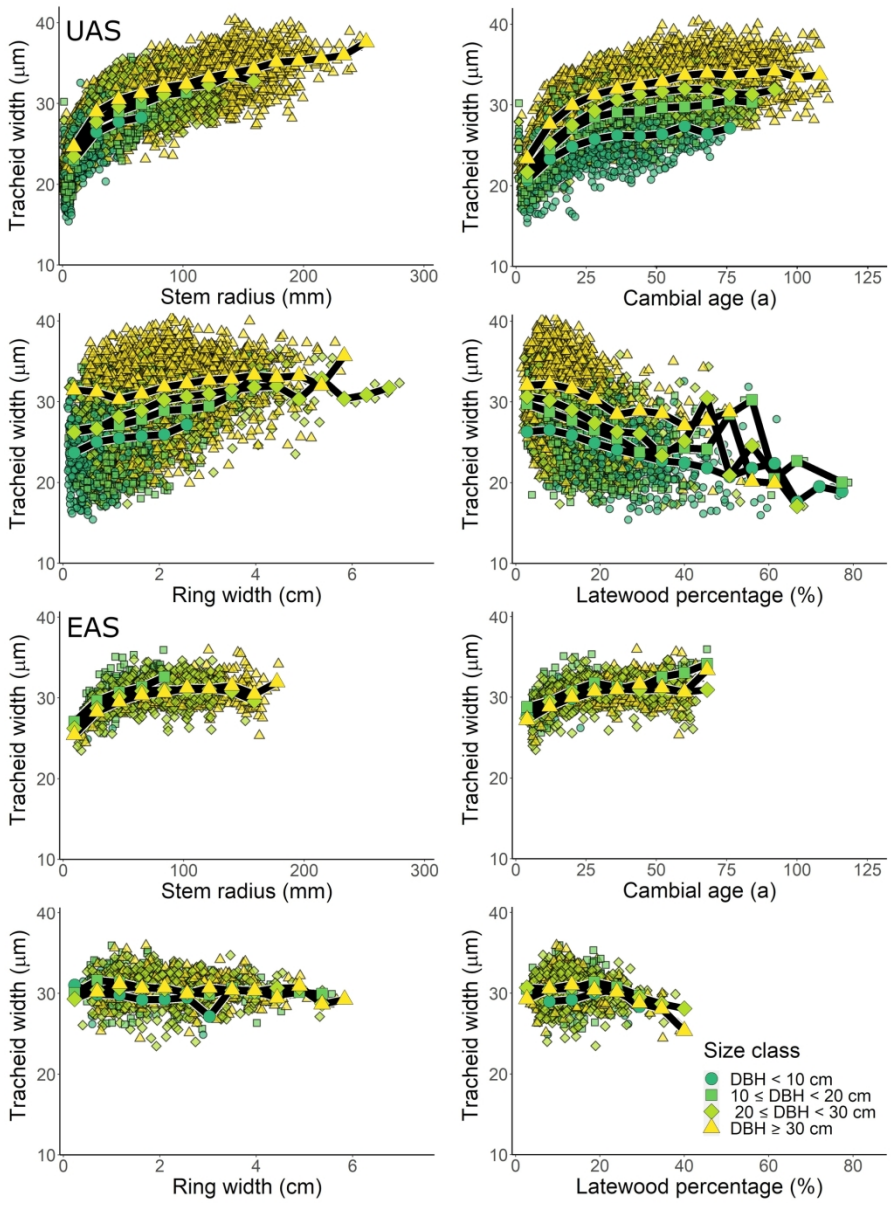

Figure 2. Observed tracheid widths in uneven-aged and even-aged stands (UAS and EAS) with respect to stem radius, cambial age, ring width and latewood percentage in the four size classes. Lines indicate class means at 15 equal intervals with respect to the x-axis. For UAS and EAS, n = 6004 and n = 1191, respectively.

176x236mm (300 x 300 DPI)

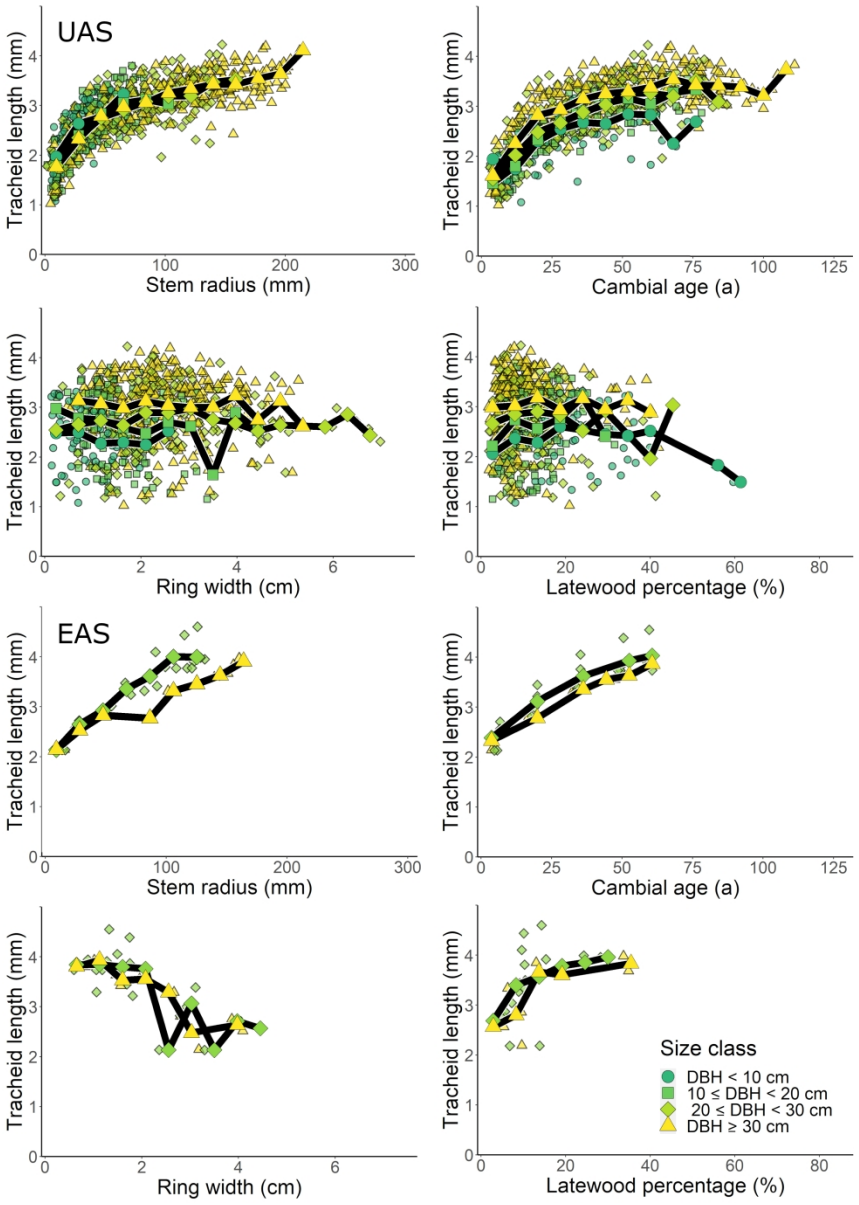

Figure 3. Observed tracheid lengths in uneven-aged and even-aged stands (UAS and EAS) with respect to stem radius, cambial age, ring width and latewood percentage in the four size classes. Lines indicate class means at 15 equal intervals with respect to the x-axis. For UAS and EAS n = 754 and n = 30, respectively.

1060x1481mm (96 x 96 DPI)

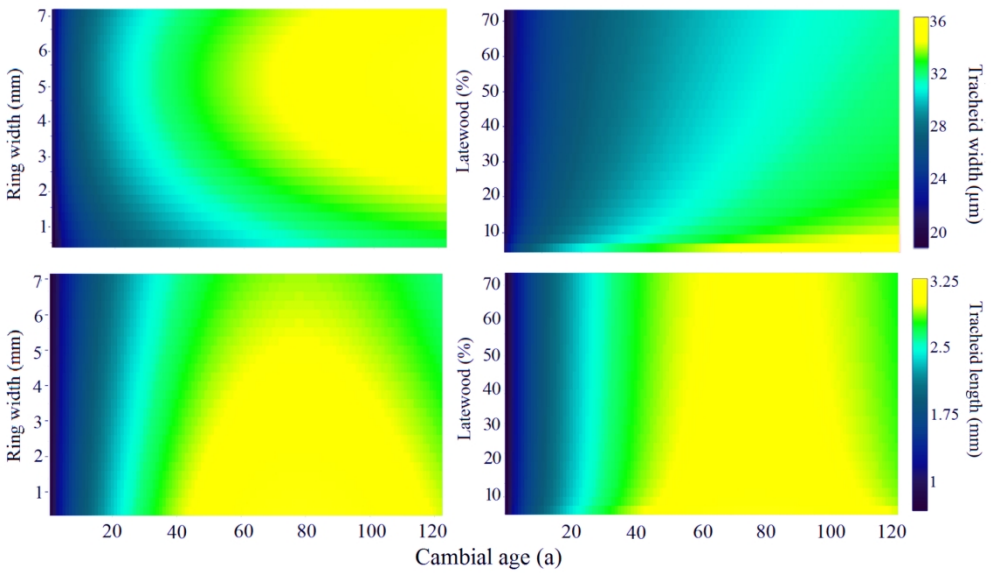

Figure 4. Predicted tracheid widths and predicted tracheid lengths in UAS trees with respect to cambial age, ring width and latewood percentage, using the models fitted to data from the UAS trees. The colors indicate the width (upper panes) and length (lower panes) of the tracheids with respect to the combined effects of cambial age (x-axis), and ring width, or latewood percentage (y-axis).

171x99mm (300 x 300 DPI)

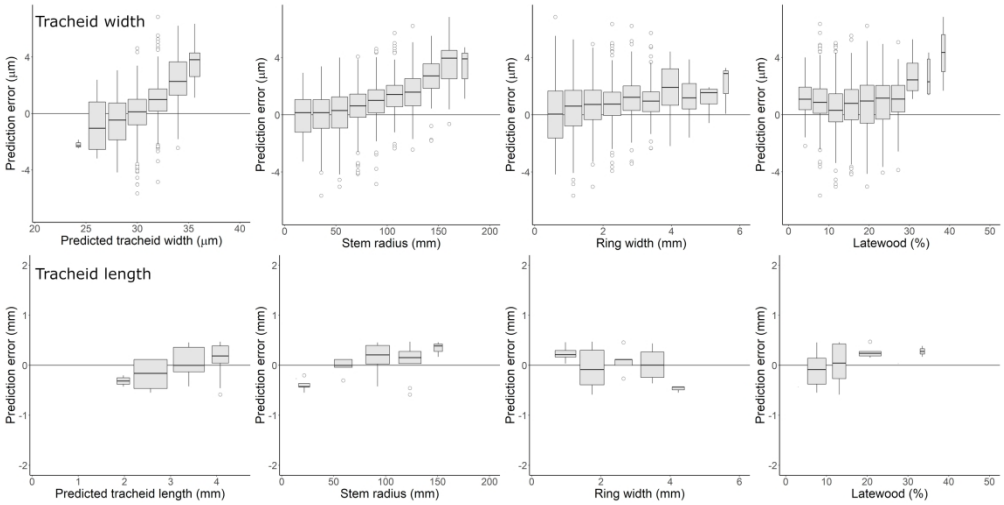

Figure 5. Prediction errors of the tracheid dimensions in even-aged stands (EAS), when EAS data are used as inputs to the models fitted to uneven-aged data. The prediction errors are given with respect to the predicted values and the fixed variables stem radius, ring width, and latewood percentages in EAS.

236x118mm (300 x 300 DPI)

Table *A1*. Pearson correlation coefficients (r) and significance levels (*p*) between key variables in the data used for modeling tracheid width.

	$Width_{ijkl}$	$WidthEW_{ijkl}$	$WidthTW_{ijkl}$	$WidthLW_{ijkl}$	$R_{ring\ ijkl}$	CA_{ijkl}	RW_{ijkl}	LWP_{ijkl}	TWP_{ijkl}
$WidthEW_{ijkl}$	0.962								
	<0.001								
$WidthTW_{ijkl}$	0.881	0.825							
	<0.001	*<0.001*							
$WidthLW_{ijkl}$	0.574	0.538	0.670						
	<0.001	*<0.001*	*<0.001*						
$R_{ring\ ijkl}$	0.765	0.769	0.707	0.503					
	<0.001	*<0.001*	*<0.001*	*<0.001*					
CA_{ijkl}	0.627	0.667	0.616	0.491	0.850				
	<0.001	*<0.001*	*<0.001*	*<0.001*	*<0.001*				
RW_{ijkl}	0.492	0.425	0.398	0.245	0.364	0.096			
	<0.001	*<0.001*	*<0.001*	*<0.001*	*<0.001*	*<0.001*			
LWP_{ijkl}	-0.445	-0.346	-0.204	0.113	-0.181	0.008	-0.497		
	<0.001	*<0.001*	*<0.001*	*<0.001*	*<0.001*	*0.527*	*<0.001*		
TWP_{ijkl}	-0.125	-0.092	0.064	0.082	-0.056	-0.077	0.203	-0.042	
	<0.001	*<0.001*	*<0.001*	*<0.001*	*<0.001*	*<0.001*	*<0.001*	*<0.001*	
dbh_{ijk}/dbh_{dom_ij}	0.588	0.554	0.493	0.292	0.584	0.317	0.499	-0.340	-0.049

<0.001	*<0.001*	*<0.001*	*<0.001*	*<0.001*	*<0.001*	*<0.001*	*<0.001*	*<0.001*

where

$Width_{ijkl}$ = Average radial tracheid width in annual ring *l* in tree *k* on plot *j* at site *i*, µm

$WidthEW_{ijkl}$ = Average radial tracheid width in latewood of annual ring *l* in tree *k* on plot *j* at site *i*, µm

$WidthTW_{ijkl}$ = Average radial tracheid width in transition wood in annual ring *l* in tree *k* on plot *j* at site *i*, µm

$WidthLW_{ijkl}$ = Average radial tracheid width in latewood in annual ring *l* in tree *k* on plot *j* at site *i*, µm

$R_{ring\ ijkl}$ = Distance from pith of annual ring *l* in tree *k* on plot *j* at site *i*, mm

CA_{ijkl} = Cambial age of annual ring *l* in tree *k* on plot *j* at site *i*, years

RW_{ijkl} = Width of annual ring *l* in tree *k* on plot *j* at site *i*, mm

LWP_{ijkl} = Latewood proportion of annual ring *l* in tree *k* on plot *j* at site *i*, %

TWP_{ijkl} = Transition wood proportion of annual ring *l* in tree *k* on plot *j* at site *i*, %

d_{ijk}/d_{dom_ij} = Relative tree diameter (stem diameter of tree k on plot j at site i divided by the average diameter of the 100 thickest trees on plot j at site i)

i ,j, k, l = indicators of hierarchy in the data: annual ring *l* in tree *k* on plot *j* at site *i*

Table *A2*. Pearson correlation coefficients (r) and significance levels (*p*) between key variables in the data used for modeling tracheid length.

	$Length_{ijkm}$	$Width_{ijkm}$	$WidthEW_{ijkm}$	$WidthLW_{ijkm}$	$R_{sample\ ijkm}$	CA_{ijkl}	RW_{ijkm}	LWP_{ijkm}	TWP_{ijkm}
$Width_{ijkm}$	0.816								
	<0.001								
$WidthEW_{ijkm}$	0.833	0.980							
	<0.001	*<0.001*							
$WidthLW_{ijkm}$	0.637	0.702	0.676						
	<0.001	*<0.001*	*<0.001*						
$R_{sample\ ijkm}$	0.754	0.784	0.796	0.611					
	<0.001	*<0.001*	*<0.001*	*<0.001*					
CA_{ijkl}	0.713	0.621	0.667	0.538	0.837				
	<0.001	*<0.001*	*<0.001*	*<0.001*	*<0.001*				
RW_{ijkm}	0.189	0.461	0.400	0.286	0.341	0.025			
	<0.001	*<0.001*	*<0.001*	*<0.001*	*<0.001*	*0.498*			
LWP_{ijkm}	-0.252	-0.485	-0.409	-0.005	-0.194	0.025	-0.563		
	<0.001	*<0.001*	*<0.001*	*0.897*	*<0.001*	*0.495*	*<0.001*		
TWP_{ijkm}	-0.205	-0.222	-0.206	0.013	-0.127	-0.193	0.200	0.097	
	<0.001	*<0.001*	*<0.001*	*0.719*	*0.001*	*<0.001*	*<0.001*	*0.009*	
dbh_{ijk}/dbh_{dom_ij}	0.369	0.534	0.508	0.365	0.511	0.241	0.438	-0.323	-0.020

<0.001	*<0.001*	*<0.001*	*<0.001*	*<0.001*	*<0.001*	*<0.001*	*<0.001*	*0.590*

where

$Length_{ijkm}$ = Average tracheid length in the 1-cm thick sample *m* in tree *k* on plot *j* at site *i*, mm

$Width_{ijkm}$ = Average tracheid radial width in the 1-cm thick sample *m* in tree *k* on plot *j* at site *i*, mm

$WidthEW_{ijkm}$ = Average tracheid radial width in earlywood in the 1-cm thick sample *m* in tree *k* on plot *j* at site *i*, mm

$WidthLW_{ijkm}$ = Average tracheid radial width in latewood in the 1-cm thick sample *m* in tree *k* on plot *j* at site *i*, mm

$R_{sample\ ijkm}$ = Distance from pith (of the edge furthest from the pith) of the 1-cm thick sample m in tree k on plot j at site i, mm

CA_{ijkl} = Cambial age of the annual ring l that lies nearest to the pith in the 1-cm thick sample *m* in tree *k* on plot *j* at site *i*, years

RW_{ijkm} = Average width of annual rings in the 1-cm thick sample *m* in tree *k* on plot *j* at site *i*, mm

LWP_{ijkm} = Average latewood proportion in annual rings in the 1-cm thick sample *m* in tree *k* on plot *j* at site *i*, %

TWP_{ijkm} = Average transition wood proportion in annual rings in the 1-cm thick sample *m* in tree *k* on plot *j* at site *i*, %

dbh_{ijk}/dbh_{dom_ij} = Relative tree diameter (stem diameter of tree *k* on plot *j* at site *i* divided by the average diameter of the 100 thickest trees on plot *j* at site *i*)

i, j, k, l or m = indicators of hierarchy in the data: sample *m* or annual ring *l* in tree *k* on plot *j* at site *i*